Dynamic Crosslinking of Thermoplastics via Nitrene C-H Insertion to Form Recyclable Thermosets

Zhi Yuan Lee, [1,5] Sirin Kamarulzaman,[1,2,5] Rizqullah Rasyiddin,[1] Sheila Y.X. Sim,[1] Georgina E.K.K. Seah, [1] Ai Wei Gan,[1] Zibiao Li,[1,,3,4] Zhuang Mao Png,[3]* and Shermin S. Goh[1,6]**

[1] Institute of Materials Research and Engineering (IMRE), Agency for Science, Technology and Research (A*STAR), 2 Fusionopolis Way, Innovis #08-03, Singapore 138634, Republic of Singapore
[2] School of Materials Science and Engineering, Nanyang Technological University, 50 Nanyang Ave, Singapore 639798, Republic of Singapore
[3] Institute of Sustainability for Chemicals, Energy and Environment (ISCE2), A*STAR, 1 Pesek Road, Jurong Island, Singapore 627833, Republic of Singapore
[4] Department of Materials Science and Engineering, National University of Singapore, 9 Engineering Drive 1, Singapore 117576, Republic of Singapore
[5] These authors contributed equally
[6] Lead contact
*Correspondence: png_zhuang_mao@isce2.a-star.edu.sg
**Correspondence: gohsms@imre.a-star.edu.sg

The Bigger Picture

Covalent Adaptable Networks (CANs) have recently seen intense research interest due to their promise as next-generation sustainable materials. Although CANs are typically synthesised from monomers, post-polymerisation functionalisation could be beneficial, especially when the monomers face compatibility issues with polymerisation conditions. This work showcases perfluorophenylazide-derived nitrene chemistry as a universal, non-specific crosslinking agent to transform a broad scope of thermoplastics, including poly(olefins), into CANs. Crosslinking with dynamic bonds imparted enhanced mechanical strength, solvent and dimensional stability, as well as self-healability and recyclability to the networks.

We envision that this strategy can be applied to develop new stimuli-responsive crosslinked materials with improved plastic circularity. Post-polymerisation functionalisation can also be applied to valorise waste plastic feedstocks, enabling recycling or upcycling efforts, thereby contributing towards United Nations Sustainable Development Goals (UN SDGs) of responsible consumption and production (UN SDG 12) and climate action (UN SDG 13).

Summary

Covalent Adaptable Networks (CANs) are polymers crosslinked *via* dynamic covalent bonds (DCB), endowing the networks with both thermoset-like stability and thermoplastic-like recyclability. Although post-polymerisation crosslinking of thermoplastics is an efficient strategy to form CANs, the process is non-trivial, especially for poly(olefins) which have low functionality and fully hydrocarbon backbone. Herein, we introduce perflurophenylazide-based nitrene crosslinkers to install disulfide, imine, and acetal DCBs into poly(olefins) and other thermoplastics, thereby converting them into CANs. Crosslinking was effective for a wide range of thermoplastics, imparting both dimensional and solvent stability. The resultant CANs could also exhibit enhanced mechanical performance, such as doubling of tensile toughness and self-healing ability. Unlike traditional thermosets, the DCBs enabled these CANs to be chemically and/or mechanically recycled multiple times. This methodology has the advantage of utilising existing and even postconsumer plastic blends as starting materials, improving their thermomechanical properties while maintaining closed-loop recyclability of these circular polymers.

Keywords: covalent adaptable networks, vitrimers, C-H functionalization, nitrene, dynamic covalent bonds, disulfide, imine, acetal

Introduction

Covalent Adaptable Networks (CANs) are a class of new-generation polymers which have the potential to combine the recyclability of thermoplastics with the superior mechanical properties of thermosets[1–3] This is achieved by their dynamic covalent bonds (DCBs), which allow for topological rearrangement mediated by exchange reactions.[4] Driven by both environmental concerns[5–8] and material properties, the field of CANs has received tremendous research interest within the last decade,[9,10] with developments expanding the scope of DCBs, polymers, starting materials, and their corresponding applications.[1,2,11] Broadly speaking, CANs can be prepared either from monomeric or polymeric starting materials. When building from monomers, crosslinks of existing thermosets can be modified to incorporate DCBs (Figure 1ai). This strategy is typified by acrylate-type polymers as well as some epoxy type polymers.[12,13] Alternatively, the DCBs can be formed during the polymerization process, and thus be directly incorporated into the backbone of the polymer network (Figure 1aii).[14,15] In recent years, there has also been interest in converting existing thermoplastics into CANs *via* a post-polymerization approach (Figure 1aiii). This approach can be advantageous in allowing the valorisation of waste plastic feedstock in either recycling or upcycling efforts, a key concern in today's world.[16,17] However, conversion of poly(olefins) into CANs is challenging due to their inert hydrocarbon structure. As such, crosslinking of poly(olefins) is typically achieved by radical-based reactive grafting using reagents such as dicumyl peroxide or maleimide crosslinkers.[18–22] Recently, taking inspiration from Wulff's group,[23,24] Chen and co-workers developed an alternate strategy to install DCBs into poly(olefins) using diazirine moieties as carbene precursors.[25] Unlike radical based chemistry, carbene C-H insertion can be tuned to proceed via its singlet state,[26] which does not typically suffer from deleterious side reactions such as chain scission.

Besides radical and carbene based chemistry, another important approach towards non-specific crosslinking is that of nitrene chemistry, with azidoformates[27] and phenyl azides[28–30] being common precursors. Decomposition of the azide first gives rise to the singlet nitrene, which can perform alkyl or aryl C-H insertion reactions.[28] However, being a highly reactive species, nitrenes are able to undergo a plethora of other reactions including ring expanded ketenimine reactions, C=C bond aziridination, or undergo intersystem crossing to transpose into its triplet state, where it can participate in radical type reactions such as proton abstraction or radical recombination reactions.[28–33] Perfluorination of the benzene ring was found to significantly increase the lifetime of the singlet nitrene and retard the competing ketenimine isomerism, thus improving C-H insertion yields.[29,30] Optimisation and design of the azide precursor allowed Ho and coworkers to utilize perfluorinated azides as highly efficient general crosslinkers in conducting polymers[31,34] and thermoelectric devices.[35] Although these crosslinkers were optimized for photo-crosslinking,[36] azides can also be thermally activated to form the reactive nitrene. Furthermore, the higher decomposition temperature of ~150 °C[34] compared to diazirines (~ 110 °C–130 °C)[37] can be advantageous in preventing premature activation during polymer pre-processing.

In this work, we demonstrate the use of perfluorophenylazides (PFPA) as nitrene precursors for *in-situ* crosslinking of thermoplastics to form CANs (Figures 1aiii, 1b).[38] Through crosslinker design, we were able to incorporate three different types of DCBs in short, high-yielding syntheses (Figure 1c). Upon thermal activation, these crosslinkers could crosslink a variety of thermoplastics, including fully hydrocarbon poly(olefins) such as poly(ethylene) (PE) and poly(propylene) (PP), demonstrating the

utility of nitrene C-H insertion as a universal crosslinking strategy. The resultant CANs demonstrated superior chemical and dimensional stability compared to the pristine thermoplastics and control polymers, while still retaining chemical recyclability. The low-density PE (LDPE)-disulfide vitrimers also exhibited intrinsic self-healing and mechanical reprocessability, as well as enhanced tensile strength and elongation relative to pure thermoplastic LDPE. Reprocessing of these vitrimers was tunable by addition of phosphine catalyst as demonstrated by small amplitude oscillatory shear (SAOS) and stress relaxation experiments. Finally, we also explored conversion of postconsumer plastics blends (LDPE/PP) into vitrimers. Excellent crosslinking efficacy was achieved even for the mixed plastics, demonstrating the potential for upcycling plastic waste.

Nitrene activation and model studies

Three different PFPA-containing crosslinkers were synthesized in 2 steps from commercially available starting materials. The disulfide (**SS**) crosslinker was synthesized from pentafluorobenzoyl chloride in 95% yield, while imine (**Im**) and spiroacetal (**SpA**) crosslinkers were synthesized from pentafluorobenzaldehyde in 67% and 77% yields respectively (Figure 1c, SI Section 2.1-2.3). Meanwhile, a static ester (**Es**) crosslinker was also synthesized as a control (SI Section 2.4). This synthetic method is highly efficient compared to aziridine-based[25] carbene precursors (39%) or azidoformate-based nitrene precursors[27] (4%) reported in literature. The PFPA group could lose N_2 when triggered by ultraviolet (UV) or thermal activation, forming a reactive nitrene species. The crosslinkers exhibited UV absorption bands between 250-280 nm (Figure S1) due to the PFPA group;[36,39] but UV activation was not pursued as we expect light penetration depth issues to limit scalability. Instead, we investigated thermolysis of the azide group via thermogravimetric analysis (TGA) and differential scanning calorimetry (DSC) to determine the activation temperature (Figures S2-4, Table S1); the results indicate that 160 °C is sufficient to fully activate the PFPA groups to form the reactive nitrene species.

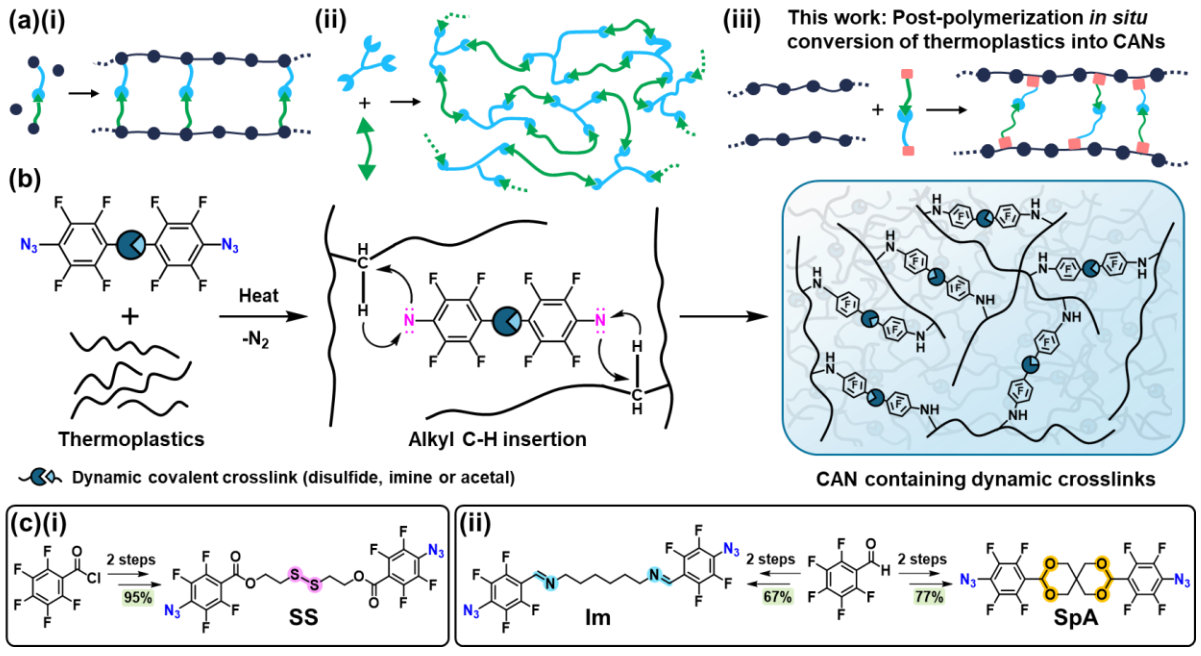

Figure 1. (a) Strategies to synthesize CANs: (i) Polymerisation of *co*-monomers containing DCBs; (ii) Polymerisation *via* formation of DCBs; (iii) Our work demonstrates the *in situ* conversion of thermoplastics into CANs using PFPA-functionalised dynamic covalent crosslinkers; (b) Thermal activation of PFPA groups form reactive nitrenes which undergo alkyl C-H insertion with thermoplastics

to form permanent amine bonds; during this process, DCBs are incorporated to form a CAN; (c) Synthesis of (i) **SS**, (ii) **Im** and **SpA** crosslinkers in 2 steps each.

The reactive nitrene species could then insert into a C-H covalent bond to give a -NH-C bond linkage (Figure 1b). This C-H insertion process is non-specific and thus high crosslinking efficiency could be achieved approaching the theoretic limit of unity, meaning that one crosslink would be formed for each crosslinker present in the matrix (at low crosslinker concentration).[36] To demonstrate that crosslinking could occur at this temperature without degradation of the crosslinker or dynamic bond, model studies were conducted using cyclohexane as a molecular model for apolar poly(olefins). For crosslinkers **SS** and **SpA**, the expected products were isolated (in 38% and 18% yield respectively) and confirmed by nuclear magnetic resonance (NMR) spectroscopy and high-resolution mass spectrometry (HRMS) (SI Section 2.8), demonstrating the potential for crosslinking aliphatic polymers such as LDPE and PP. Besides the expected C-H insertion product, the nitrene reaction (especially via thermal activation) is also known to be complex, giving rise to other side products such as ketenimines (via ring expansion), azobenzenes, and other radical reaction pathways (Scheme S5).[28–33] Meanwhile, crosslinker **Im** gave a low yield (<6%) with a mixture of various fluorinated products. This could be due to facile hydrolysis of the imine bond,[40] releasing free amines that could undergo side reactions such as nucleophilic aromatic substitution. Thus, recycling of the networks crosslinked with **Im** was not investigated.

Crosslinking thermoplastics to form CANs

We examined the scope of possible thermoplastics by reacting our 3 different crosslinkers with apolar commodity poly(olefins) such as LDPE and PP, and polar biocompatible polymers such as poly(ethylene oxide) (PEO) and poly(caprolactone) (PCL). The thermoplastics were dissolved in hot solvents, followed by the addition of crosslinker with stirring and removal of solvent at 100 °C under a stream of nitrogen. The temperature was kept below the PFPA activation temperature to prevent formation of nitrene, which might react with the remaining solvent and lead to reduced crosslinking efficiency. Subsequently, the polymer was dried at 110 °C under vacuum and then temperature was raised to 160 °C for 10 hr to enable thermally activated crosslinking. Using this strategy, various thermoplastics were crosslinked with either **SS**, **Im** or **SpA** at different weight percentages (wt%) with respect to the polymer weight. Post-crosslinking, the polymer networks turned dark brown. This may be attributed to the formation of side products of nitrene chemistry, such as azobenzenes, ketenimines, and their related products, which are known to be deeply coloured.[28–33]

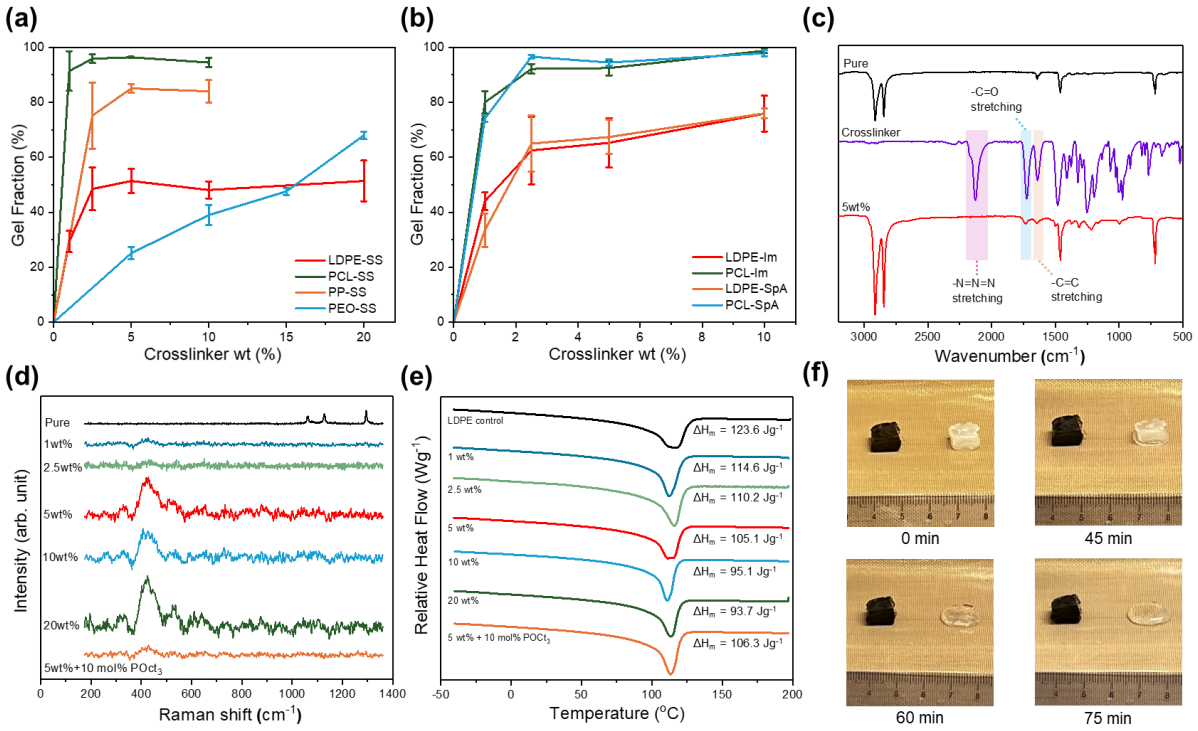

Figure 2. Gel fraction of (a) **SS**, (b) **Im** and **SpA**-crosslinked thermoplastics as a function of increasing crosslinker wt%; (c) FTIR spectroscopy of pure LDPE, **SS** crosslinker and **LDPE-SS-5** demonstrate successful C-H insertion of **SS** crosslinker into LDPE polymer; (d) Raman spectroscopy of **LDPE-SS-X** exhibit increasing S-S vibrations with increasing crosslinker wt%; (e) DSC curves of **LDPE-SS-X** exhibit decreasing ΔH_m with increasing crosslinker wt%; (f) Photographs demonstrate that **LDPE-SS-5** (left) retains its shape while pure LDPE samples (right) melt when heated to 130 °C on a hot plate.

Gel fraction tests were used to measure the degree of crosslinking for the various CANs. Focusing on the polymers crosslinked with **SS**, high gel fractions were observed for PP and PCL polymers (>85%) with just 5 wt% **SS** added, indicating good crosslinking efficacy (Figure 2a). For LDPE, a low gel fraction of 33 ± 6% was obtained with 1 wt% **SS**, which increased to 49 ± 8% at 2.5 wt%. However, there was no significant increase in gel fraction even up to 20 wt% **SS** (51 ± 7%). Compared with PP, this observation may be attributed to the higher degree of branching of LDPE, which potentially increases the probability of C-H insertion occurring within the same polymer molecule instead of between different molecules, resulting in a lower gel fraction. For **Im** and **SpA** crosslinkers, a trend of increasing gel fraction with higher wt% crosslinker was observed for all crosslinked polymers (Figures 2b, S5-6). The control static **Es** crosslinker could crosslink LDPE as well, yielding a gel fraction of 76.5% at 5 wt% loading. The appearance of strong C=O stretching (1725 cm^{-1}) and C=C stretching (1640 cm^{-1}) peaks and the disappearance of the azide stretching (2128 cm^{-1}) peak in the Fourier Transform Infrared Spectroscopy (FTIR) spectra of **LDPE-SS-X** (LDPE crosslinked with X wt% **SS**) indicated successful activation of PFPA and insertion of **SS** crosslinker into the polymer (Figures 2c, S7); similar results were observed with other polymers and crosslinkers (Figures S8-10, 14-17). Raman spectroscopy of **LDPE-SS-X** indicated the disappearance of crystalline LDPE peaks after crosslinking. For the peak corresponding to disulfide bonds (425 cm^{-1}), a clear increase in intensity with crosslinker loading was also observed (Figure 2d).[41] TGA graphs of various networks with different crosslinkers also showed that the polymers displayed good thermal stability with thermal decomposition temperatures above 300 °C (Figures S19-24, 27-30). DSC curves of the polymers did not show significant changes in melting point (T_m), while the enthalpy of fusion (ΔH_m) was observed to decrease with increasing crosslinker loading (Figures S32-35, 39-42). Citing **LDPE-SS-X** CANs as an example (Figure 2e), the ΔH_m of **LDPE control** (treated in the same manner as **LDPE-SS-X** except without

addition of crosslinker), 123.6 J g^{-1}, decreased to 93.7 J g^{-1} for **LDPE-SS-20**. Crosslinked regions are non-melting as they become more thermoset-like, resulting in a decrease in ΔH_m.[23,24] Additionally, X-ray diffraction (XRD) experiments showed a slight decrease in crystallinity with increasing crosslinker density (from 43.6% in **LDPE control** to 39.5% in **LDPE-SS-20,** Figures S44-47, Table S2), which may also contribute towards the decrease in ΔH_m.[42]

As we are interested in the potential of transforming single-use commodity poly(olefins) into durable, recyclable thermosets to alleviate plastic waste,[18,21,43,44] we focus on LDPE as the thermoplastic backbone for further experiments. To minimise the amount of crosslinker used, we chose to investigate **LDPE-SS-5** for subsequent rheology and mechanical analysis. Although the gel fraction of **LDPE-SS-5** is relatively lower than other crosslinked polymers with 5 wt% **SS**, the polymer displayed excellent dimensional stability when heated above the T_m of LDPE (Figure 2f). While the pure LDPE cube completely melted within 75 min at 130 °C, the **LDPE-SS-5** cube still retained its structure with no significant change in shape, demonstrating that the current degree of crosslinking is sufficient to maintain a stable network structure even above T_m.

Vitrimeric properties of LDPE-SS-5

Disulfide dynamic bond exchanges have been shown to occur via several pathways, including associative, metathesis and dissociative mechanisms, mediated by free thiols, thiolates or sulfenyl radicals.[45–47] We performed rheological analysis[48–50] to study the impact of catalyst on the viscoelastic performance of **LDPE-SS-5** and its analogue **LDPE-SS-5-POct$_3$**, which contains 10 mol% trioctylphosphine ($POct_3$). Temperature ramp experiments showed that addition of $POct_3$ altered the reaction mechanism: for uncatalyzed **LDPE-SS-5**, storage modulus (G') decreased by a magnitude of 2 while the G' of **LDPE-SS-5-POct$_3$** decreased by a magnitude of 3 over the same temperature range (100-200 °C) (Figures 3a-b, S51). Additionally, while loss factor remained low for **LDPE-SS-5** (tan(delta) ≤ 0.5), it increased steadily for **LDPE-SS-5-POct$_3$** when heated above 120 °C to eventually reach tan(delta) ~ 1 at about 200 °C, suggesting a decreasing crosslink density for **LDPE-SS-5-POct$_3$**, which is characteristic of a dissociative mechanism.[46] The mechanism likely involves nucleophilic attack of the organophosphine on a sulfur centre, thus cleaving the disulfide bonds to form thiolate anions and promotes disulfide exchange.[51–53] This may also account for the lower gel fraction of **LDPE-SS-5-POct$_3$** (38 ± 6%) and the lower intensity of the S-S peak in the Raman spectrum (Figure 2d) in comparison to **LDPE-SS-5**.

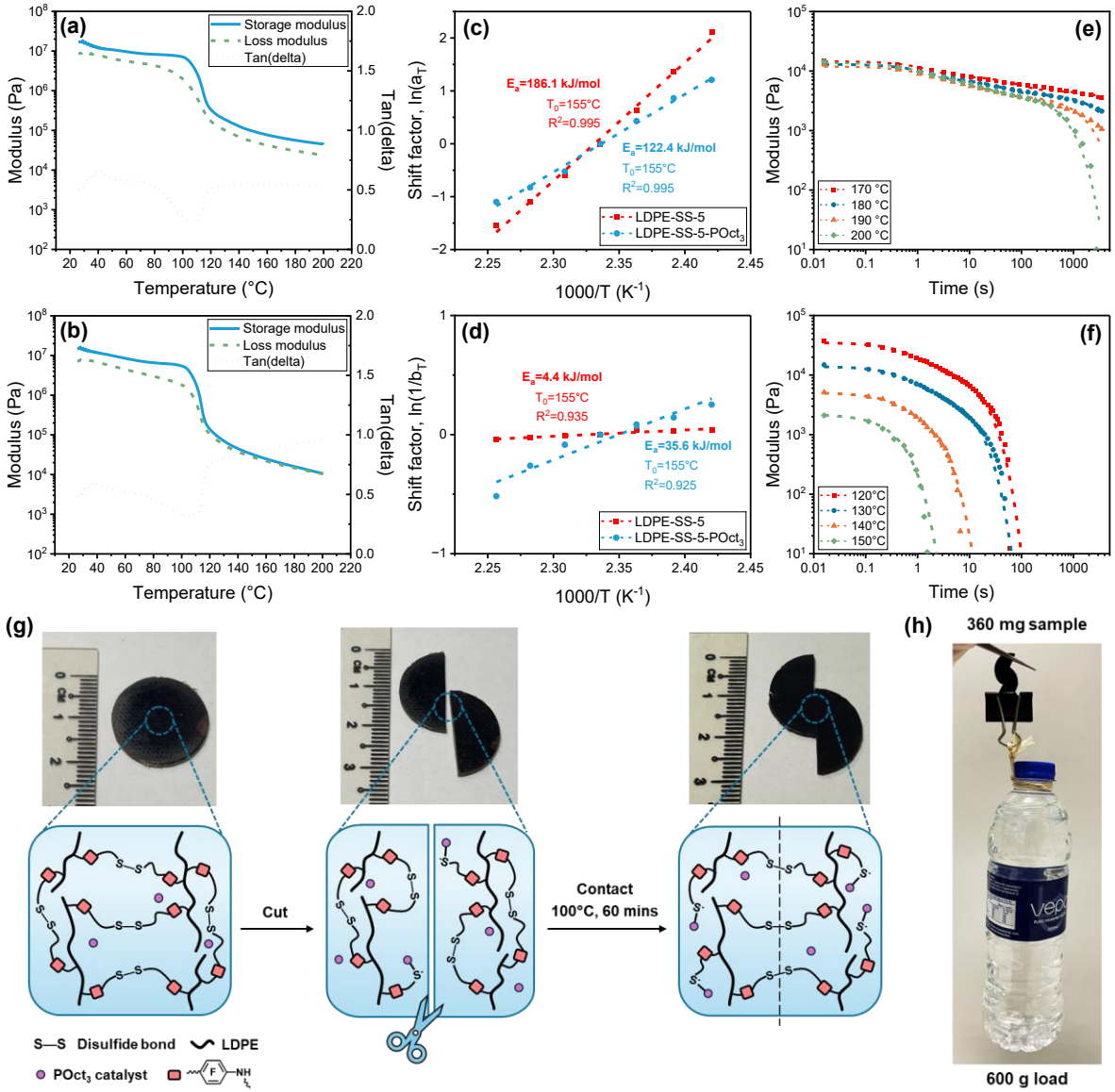

Figure 3. (a-b) Storage (G') and loss (G") modulus and tan(delta) as a function of temperature for **LDPE-SS-5** and **LDPE-SS-5-POct$_3$** respectively; (c-d) Arrhenius plot of TTS shift factors a_T and ($1/b_T$), respectively, against 1000/T for **LDPE-SS-5** and **LDPE-SS-5-POct$_3$**; (e-f) Stress relaxation experiments and Maxwell fitting (dotted lines) for **LDPE-SS-5** (3-element) and **LDPE-SS-5-POct$_3$** (2-element) respectively demonstrate the decreased relaxation time upon addition of $POct_3$; (g) Illustration and photographs of the self-healing process of **LDPE-SS-5-POct$_3$** polymer; (h) Photograph of the healed **LDPE-SS-5-POct$_3$** polymer holding a water bottle (600 g).

Further investigations by SAOS experiments (0.1-10 Hz) demonstrated that addition of $POct_3$ also lowered the activation energy (E_a) of the reaction. Within the temperature range of 140-170 °C, **LDPE-SS-5** did not exhibit a crossover and behaved as a viscoelastic solid throughout this range, while **LDPE-SS-5-POct$_3$** transitioned to a viscous liquid more rapidly as temperature increased, again indicative of dissociative behaviour (Figures S52a-b). Time-temperature superposition (TTS) was performed on frequency sweeps (0.1-10 Hz) with 155 °C as the reference temperature. This method involved shifting of the curves by a horizontal shift factor (a_T) to enable the curves to match. Typically, a higher temperature is shifted to lower frequencies, while a lower temperature is shifted to higher frequencies to obtain a master curve of the superimposed graphs (Figures S52c-d). The shift factors could be fitted to the Arrhenius equation, affording E_as of 186.1 and 122.4 kJ mol^{-1} for **LDPE-SS-5** and **LDPE-SS-5-POct$_3$** respectively (Figure 3c), which are consistent with literature values.[45,46] A vertical shift factor

(b_T) may also be applied; Drockenmuller et al. proposed this to be especially important for dissociative CANs to account for changes in crosslink density and G'.[54] As expected, the ($1/b_T$)-derived E_a for **LDPE-SS-5** was 4.40 kJ mol^{-1}, indicating negligible network dissociation, while for **LDPE-SS-5-POct$_3$** it was 35.6 kJ mol^{-1}, indicating that network dissociation increased with temperature (Figure 3d).

Finally, stress relaxation experiments measured over a longer duration (up to 5000 s) revealed that **LDPE-SS-5** was not rheologically simple – a 2-stage stress relaxation was observed with a distinct transition (Figure 3e).[55] The data was global fitted to the 3-element Maxwell model (Figure S52e, Table S3), which could be attributed to rapid polymer chain segmental motion, as well as disulfide bond exchange and crosslink mobility at longer timescales.[49,50] The increase in reaction rate upon addition of catalyst was evident from the dramatic decrease in stress relaxation time for **LDPE-SS-5-POct$_3$** (Figure 3f). Due to decreases in initial moduli with increasing temperature, these curves were individually fitted, rather than global fitted, to a 2-element Maxwell model (Figure S52f, Table S4), representing rapid polymer chain segmental mobility and a slightly slower disulfide bond exchange coupled with network dissociation.[54] At 150 °C, the curve collapsed to fit a 1-element model, which was supported by SAOS experiments indicating that loss modulus (G") > G' (Figure S41b). The significantly shorter relaxation time for **LDPE-SS-5-POct$_3$** arose not only from the increase in rate of disulfide bond exchange due to catalysis, but also because of higher crosslink mobility from network dissociation.

Since rheological analysis demonstrated that disulfide bond exchange could take place at elevated temperatures, we proceeded to investigate the self-healing and recyclability of these vitrimers. A **LDPE-SS-5-POct$_3$** polymer sample (thickness: 1 mm; width: 20 mm; 0.36 g) was cut and the broken pieces were gently contacted followed by heating at 100 °C for 60 min (Figure 3g). The broken interfaces recombined due to the disulfide exchange catalysed by $POct_3$, and the healed sample could hold a weight of 600 g, more than 1500 times its own (Figure 3h).

Mechanical reprocessibility of LDPE-SS-5

The tensile properties of **LDPE-SS-5** were compared against **LDPE control** (Figures 4b-c, Tables S5-6, Figures S55-56). Upon incorporation of the **SS** crosslinker, the Young's modulus decreased significantly from 309 ± 34 MPa (**LDPE control**) to 170 ± 28 MPa (**LDPE-SS-5**). This may be attributed to the decreased crystallinity of the polymer upon crosslinking, resulting in lower rigidity. We observed significant improvements in maximum elongation (91 ± 48% to 161 ± 25%) and subsequently toughness (9.9 ± 4.9 J m^{-3} to 15.8 ± 2.8 J m^{-3}) of the vitrimer network. Due to the strong covalent bonds and robust crosslinking present in the network, the vitrimer could withstand greater stress and undergo more deformation before breaking. The improved extensibility of **LDPE-SS-5** indicate the functional utility of crosslinking commodity thermoplastics with the **SS** crosslinker.

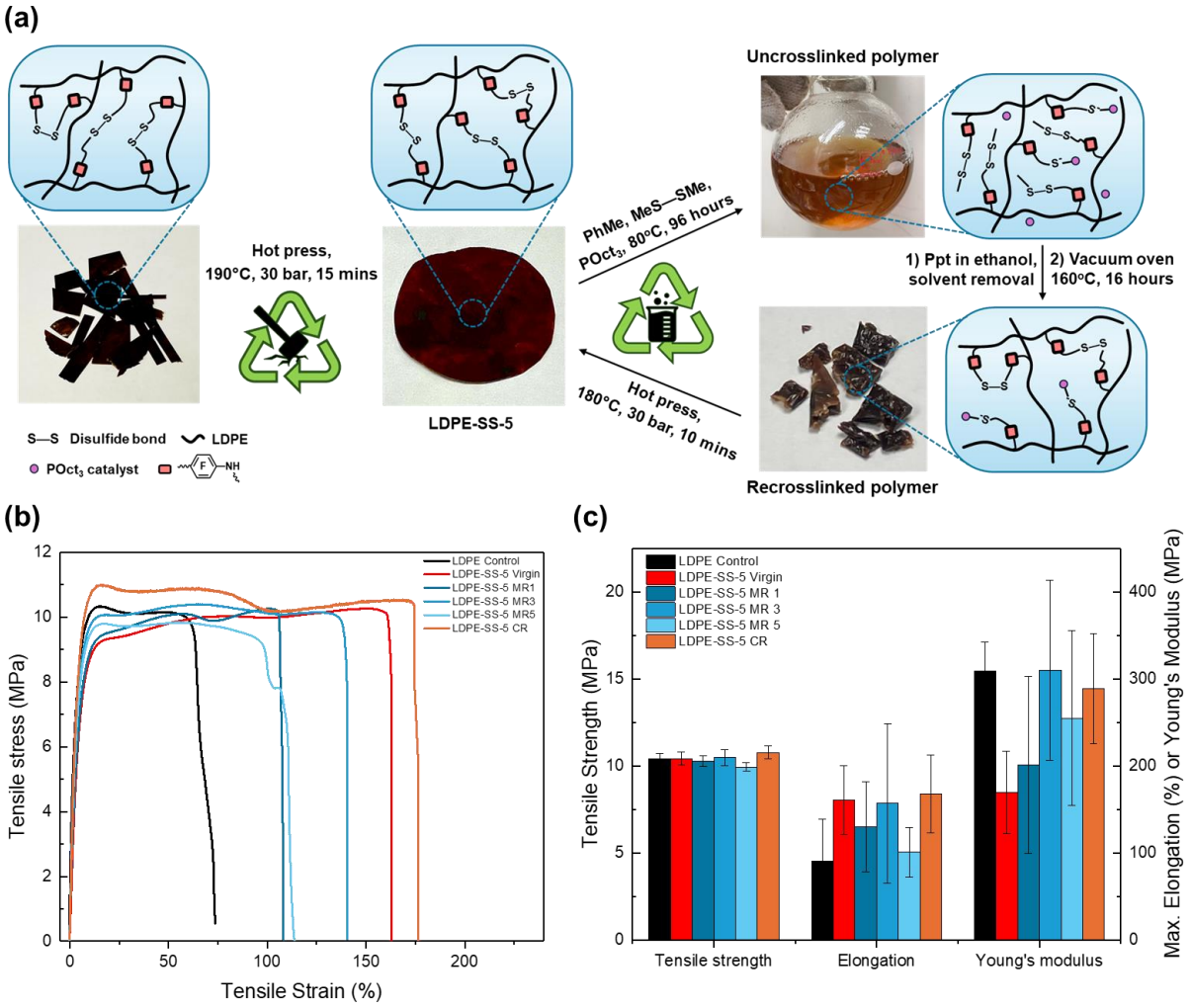

Figure 4. (a) Illustration and photographs of mechanical and chemical recycling processes of **LDPE-SS-5**; (b-c) Representative tensile stress-strain curves and a comparison plot of tensile strength, elongation and Young's modulus, respectively, for **LDPE control** and **LDPE-SS-5**, virgin (as-synthesised) and after 1, 3, and 5 mechanical recycles, or 1 chemical recycle demonstrate the recyclability of **LDPE-SS-5**.

To demonstrate the reprocessability of the vitrimer, **LDPE-SS-5** was cut into small pieces and hot-pressed (Figure 4a). A homogeneous film was obtained after hot-pressing at 190 °C, 30 bar for 15 minutes due to the exchange of the dynamic disulfide bonds at elevated temperatures. In contrast, control **LDPE-Es-5** with the static crosslinker could not be reprocessed at this temperature. After the first cycle of mechanical recycling (MR1), **LDPE-SS-5-MR1** exhibited similar tensile performance to the virgin **LDPE-SS-5** (Figures 4b-c, Table S7, Figure S57). However, after 5 cycles of mechanical recycling (MR5), **LDPE-SS-5-MR5** showed a decrease in tensile strength (9.9 ± 0.3 MPa), toughness (8.9 ± 2.9 J m^{-3}), and maximum elongation (101 ± 28%), with an increase in Young's modulus (255 ± 39 MPa) compared to **LDPE-SS-5** (Figures 4b-c, Table S9, Figure S59). The increase in stiffness and decrease in ductility of the vitrimer indicate a decrease in crosslinking density, which was supported by a decrease in gel fraction in **LDPE-SS-5-MR5** (31 ± 3%) compared to the virgin **LDPE-SS-5** (51 ± 4%) (Figure S53). The decrease in mechanical performance may be due to unwanted side reactions occurring during extended periods of heating. Although isothermal TGA experiments showed no mass loss at 190 °C over 2 hr (Figure S20), other degradative pathways which do not result release volatile molecules could occur.[59–61] The homolytic cleavage of S-S bond or C-S bond activated by heat could create reactive sulfur or carbon radicals, leading to the formation of unreactive sulfur compounds or

polysulfides, thus lowering the crosslinking density.[56] Additionally, thermo-mechanical and thermo-oxidative degradation occurring during the hot-pressing process could result in chain scission of the polymer network.[57,58] Furthermore, when the polymer is subjected to excessive stress, its network might undergo mechanochemical degradation or morphological changes, thus affecting its tensile properties.[57] Nevertheless, **LDPE-SS-5-MR5** still has higher elongation at break compared to the **LDPE control**.

Chemical recycling of CANs

We also explored the chemical recyclability of the crosslinked polymers. Typically, chemical recycling of CANs involves degradation of the network into its constituent monomers, which are then separated and purified before being recombined to resynthesize the CAN. In contrast, complete breakdown and separation of the network is not necessary in our systems. Here, the polymer backbone, and even the amine bonds formed between the reactive PFPA ends of the crosslinkers and the thermoplastic, remain untouched in our systems. Instead, bond cleavage takes place at the dynamic bonds in the centre of the crosslinker, affording soluble, un-crosslinked functionalized thermoplastic. This thermoplastic can simply be dried, remoulded, and then cured *in vacuo* to reform the CAN in its desired shape.[62]

*Chemical recycling of **LDPE-SS-5***

The chemical recyclability of **LDPE-SS-5** was investigated using dimethyl disulfide as the de-crosslinking reagent and hot toluene (80 °C) as solvent for the LDPE backbone. Dynamic exchange between dimethyl disulfide and the disulfide bond in **LDPE-SS-5** resulted in network degradation to form soluble, un-crosslinked polymer chains. In the presence of $POct_3$ (500 mol%), which was used to catalyse stress relaxation of the vitrimer, a clear brown solution was obtained after 96 h with no observable undissolved polymer pieces (Figure 4a), indicating that de-crosslinking was complete. In contrast, in the absence of the catalyst, the vitrimer remained as a swollen gel even after 168 h. The un-crosslinked polymer was retrieved by precipitation in ethanol, centrifugation to remove the excess reagents, followed by drying at 110 °C. No gel fraction was observed for the un-crosslinked polymer, as expected (Figure S54). The T_m and ΔH_m of the un-crosslinked polymer are higher (111.7 °C, 124.3 J g^{-1}) compared to **LDPE-SS-5** (111.0 °C, 105.1 J g^{-1}), presumably due to decrease in non-melting thermoset-like regions (Figure S37).

The un-crosslinked polymer was then placed in a vacuum oven at 160 °C to reform the vitrimer network (Figure 4a). Dynamic disulfide exchange reformed the disulfide bond in the crosslinkers, with concomitant expulsion of dimethyl disulfide, which was removed by vacuum, thus driving the re-crosslinking reaction. The re-crosslinked CAN (**LDPE-SS-5-CR**) had a gel fraction of 30 ± 3%, which was significantly lower than that of the original **LDPE-SS-5** (51 ± 4%), indicating that the network has a lower degree of crosslinking than before (Figure S54). The increased ΔH_m of **LDPE-SS-5-CR** (107.3 J g^{-1}) compared to **LDPE-SS-5** (105.1 J g^{-1}) also indicated a decreased crosslink density (Figure S37). These values match those obtained for the sample with 10 mol% $POct_3$, **LDPE-SS-5-POct$_3$** (38 ± 6%, 106.3 J g^{-1}), suggesting that there may be catalyst from the de-crosslinking reaction remaining in the reformed vitrimer. The FTIR spectra of the un-crosslinked, and re-crosslinked polymers did not show significant difference from the original **LDPE-SS-5** vitrimer (Figure S12).

The tensile strength (10.8 ± 0.4 MPa), maximum elongation (168 ± 45%), and toughness (16.9 ± 4.2 J m^{-3}) of **LDPE-SS-5-CR** matched those of the virgin **LDPE-SS-5** (Figures 4b-c, Table S10, Figure S60). Additionally, the Young's modulus increased significantly by 70% to 289 ± 63 MPa, presumably attributed to the increase in crystallinity after chemical recycling. Despite the decrease in crosslinking density compared to the virgin **LDPE-SS-5**, the improved mechanical performance could be attributed

to a more homogeneous crosslinking distribution within the **LDPE-SS-5-CR** network. The formation of the virgin **LDPE-SS-5** is governed by kinetics due to the rapid C-H insertion of the reactive nitrenes upon activation, which could result in uneven crosslink distribution due to factors such as phase separation between the LDPE and the **SS** crosslinker while the solvent was being removed. Issues such as trapped entanglements, elastically ineffective chains, and connectivity defects could further diminish the mechanical properties of **LDPE-SS-5**.[63] These issues may not be resolved during mechanical recycling since the vitrimer does not flow, so disulfide bonds can only rearrange with reactive moieties in close proximity, keeping the network kinetically trapped.[64] In contrast, during chemical recycling, the dissolution of the LDPE backbone in toluene allows larger scale motion of the chains which could prevent chain overlapping and inhibit trapped entanglements.[63] The covalent attachment of **SS** moieties to the polymer backbone would also minimise phase separation.[62] Additionally, due to the reversible nature of the disulfide bond, the reformation **LDPE-SS-5-CR** is thermodynamically controlled,[64] potentially enabling crosslinked regions to become more evenly distributed. Thus, chemical recycling is an effective method to restore and even improve the mechanical properties of **LDPE-SS-5**.

*Chemical recycling of **LDPE-SpA-5***

Acetal dynamic bond exchange has been shown to occur through various mechanisms, such as transacetalization,[65] acetal metathesis[66] or dissociative mechanisms via aldehydes,[14] vinyl ethers,[67,68] or carbocations.[69] In particular, the spirocyclic acetal motif in the centre of our **SpA** crosslinker resembled the 3,9-divinyl-2,4,8,10-tetraoxaspiro[5.5]undecane crosslinker used in catalyst-free metathesis of spirocyclic acetal CANs,[66] suggesting that mechanical recycling would be facile. Unfortunately, our efforts to achieve mechanical recycling of **LDPE-SpA-5** proved unsuccessful. This may partially be attributed to the basic amine group formed during the crosslinking reaction since trace amounts of base was found to supress acid-catalysed acetal metathesis.[66] However, our small molecule model exchange studies showed that analogues of **SpA** with the perfluorinated benzaldehyde moiety could not undergo acetal metathesis or dissociation even with addition of superstoichiometric amounts of acid except in the presence of alcohol (SI Section 2.9). These results are in line with the study by Lemcoff and Fuchs, which showed that electron-donating groups on acetals favour dissociation while electron-withdrawing groups do not.[65]

Nevertheless, our results demonstrated that transacetalization could occur in the presence of ethanol (SI Section 2.9), and we proceeded to investigate chemical recycling of **LDPE-SpA-5**. While previously reported chemical recycling methods for polymer networks containing acetal bonds utilised an acidic water/organic solvent mixture,[70,71] we chose to perform ethanolysis of our CAN in heated toluene (95 °C) as it effectively swelled the LDPE backbone. With *p*-toluenesulfonic acid (*p*-TsOH) as the catalyst, **LDPE-SpA-5** was successfully de-crosslinked over 24 h, as observed by a clear yellow solution obtained without any visible undissolved polymer pieces (Figure 5a). After solvent removal, a gel fraction of 51 ± 6% was obtained. Since the un-crosslinked polymer should have no gel fraction, this indicated that some re-crosslinking had occurred. This was expected since pentaerythritol, which was not removed from the reaction mixture, could transacetalise the diethyl acetal, releasing volatile ethanol which was then driven off by heat, thus facilitating re-crosslinking.

At this stage, due to the low gel fraction, the network can be hot-pressed, turning from yellow to dark brown during the process, presumably due to increased density of the polymer via compactification and/or further reactions involving the nitrene side products (Figure 5a). The gel fraction of the polymer further increased to 56 ± 2% after hot-pressing and 72 ± 3% after re-crosslinking *in vacuo*, which matched that of virgin **LDPE-SpA-5** (73 ± 8%) (Figure S61). This is expected since the extent of

crosslinking would increase with the length of exposure to high temperature. The FTIR spectra of the un-crosslinked, hot-pressed, and re-crosslinked polymer matched that of the virgin **LDPE-SpA-5**, with the exception of new peaks from *p*-TsOH (1035, 1010 cm^{-1}) (Figure S18). The T_m and ΔH_m of the un-crosslinked polymer are higher (112.3 °C, 136.0 J g^{-1}) compared to **LDPE-SpA-5** (108.7 °C, 100.1 J g^{-1}) (Figure S43), presumably since the decrease in crosslinking density within the network decreased the amount of non-melting regions. Upon re-crosslinking of the polymer, the T_m and ΔH_m decreased to 110 °C and 118.1 J g^{-1} respectively (Figure S43), indicating the polymer becoming more thermoset-like within the network due to the reformation of the acetal bonds.

The mechanical properties of the re-crosslinked polymer (**LDPE-SpA-5-CR1**) were evaluated (Figure 5b, Table S11, Figure S62). Compared to the **LDPE control**, the **LDPE-SpA-5-CR1** CAN showed a slight decrease in tensile strength (8.7 ± 0.5 MPa) and maximum elongation (46 ± 13%), which suggested a brittle polymer. Yet, **LDPE-SpA-5-CR1** possessed a higher Young's modulus (245 ± 65 MPa) than **LDPE-SS-5**, which may be attributed to the rigid spirocyclic structure of the **SpA** crosslinker, and thus could be preferred for applications where resistance to both solvent and deformation is crucial. After another chemical recycle, while the tensile strength and Young's modulus of the **LDPE-SpA-5-CR2** changed slightly, there was a significant decrease in maximum elongation (Figure 5b, Table S12, Figure S63). As the chemical recycling process is similar to that **LDPE-SS-5**, we expect that the homogeneity of crosslinked regions could similarly increase with each chemical recycle.[63,64] However, due to the rigidity of the **SpA** crosslinker as opposed to the flexibility of the **SS** crosslinker, this may have resulted in increased brittleness of the network.

Overall, both **LDPE-SS-5** and **LDPE-SpA-5** CANs could be chemically recycled via a reactive solvent-based approach. Owing to the dynamic nature of the dynamic **SS** and **SpA** bonds, the CANs were first degraded into un-crosslinked polymer chains, followed by re-crosslinking to reform the network polymers. In particular, the chemically recycled **LDPE-SS-5-CR** showed improved mechanical strength compared to the virgin CAN.

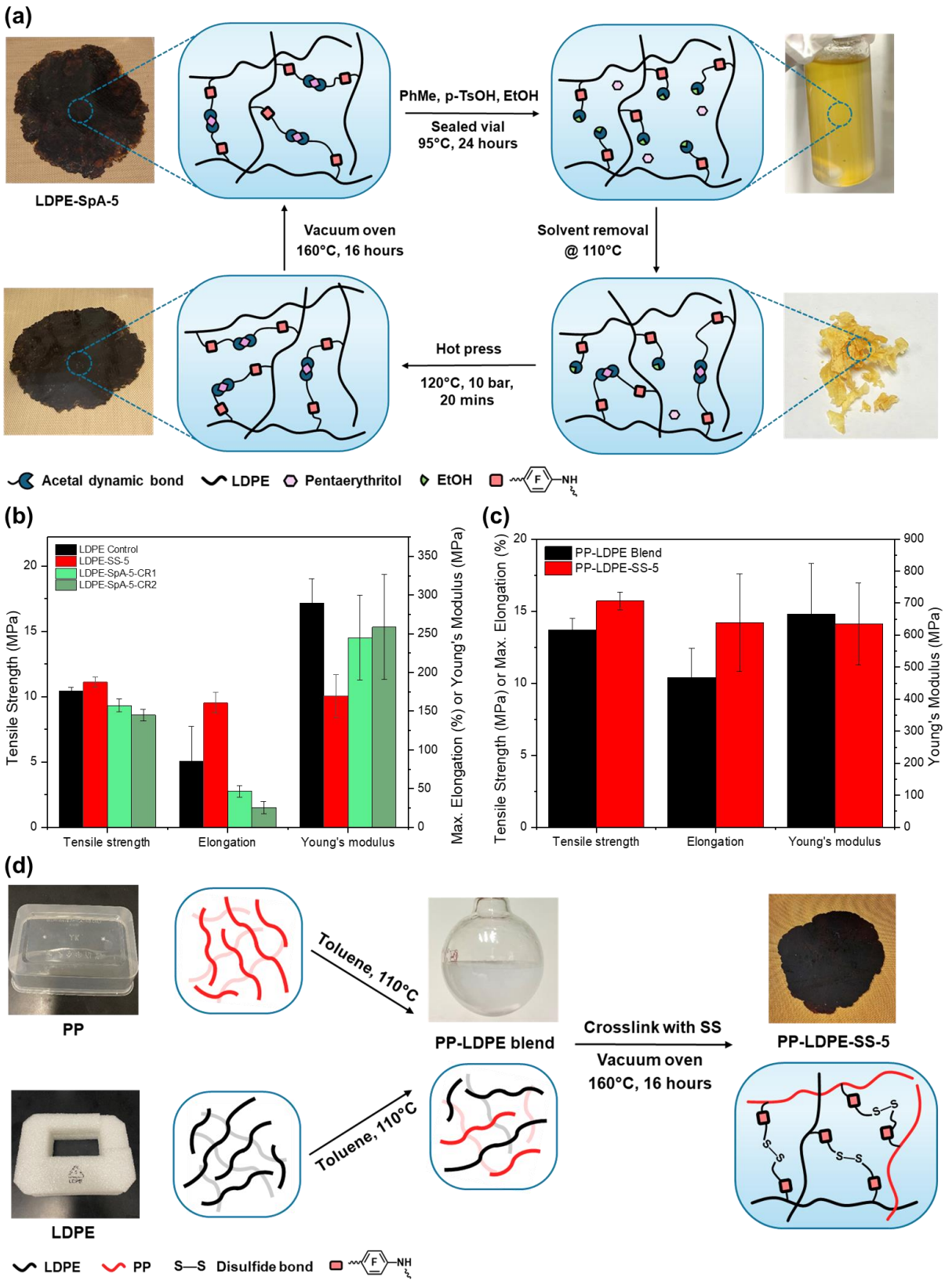

Figure 5. (a) Illustration and photographs of the chemical recycling process of **LDPE-SpA-5**; (b) Comparison of tensile strength, elongation and Young's modulus of **LDPE control**, **LDPE-SS-5**, **LDPE-SpA-5-CR1** and **LDPE-SpA-5-CR2**; (c) Comparison of tensile strength, elongation and Young's modulus of **PP-LDPE blend** and **PP-LDPE-SS-5**; (d) Illustration and photographs of preparation of **PP-LDPE blend** from LDPE packaging foam and PP food container, and crosslinking with **SS** to form **PP-LDPE-SS-5**.

Upcycling post-consumer LDPE and PP with SS crosslinker

In addition to crosslinking virgin thermoplastics, our dynamic crosslinkers can also be used to crosslink a blend of post-consumer waste, giving second (or more) life to waste plastics.[25,44] PP and PE constitute about 50% of the world's polymer production, and current recycling technology is still unable to transform such blends for high-value applications.[43,72] A polyolefin blend of LDPE and PP (70:30 w/w), a ratio commonly observed in post-consumer waste,[73] was prepared from used LDPE packaging foam and PP food container by dissolving and mixing in hot toluene (110 °C). This mixture was either dried to obtain **PP-LDPE blend** or crosslinked with 5 wt% **SS** crosslinker to obtain **PP-LDPE-SS-5** (Figure 5d). **PP-LDPE-SS-5** exhibited a gel fraction of 77 ± 3% compared to 0% for the pure **PP-LDPE blend**, indicating a relatively high degree of crosslinking within the PP and LDPE chains individually, as well as at the interfaces between the 2 different chains. Two different T_m were observed (106.3 °C and 155.3 °C) for the LDPE and PP polymer chains respectively (Figure S38). The ΔH_m for both melting transitions in **PP-LDPE-SS-5** (64.5 J g^{-1} and 21.65 J g^{-1} for PE and PP melting respectively) are lower than that of the **PP-LDPE blend** (77.9 J g^{-1}, 23.4 J g^{-1}), confirming that successful crosslinking had occurred (Figure S38). A comparison between the FTIR spectra of **PP-LDPE-SS-5** and **PP-LDPE blend** also confirmed incorporation of the crosslinker (Figure S13).

Tensile measurements showed that the **PP-LDPE-SS-5** CAN displayed enhanced mechanical properties compared to the **PP-LDPE blend** (Figure 5c, Tables S13-14, Figures S64-65), such as greater tensile strength (15.7 ± 0.6 MPa) and maximum elongation (14 ± 4%), indicating a mechanically stronger and more ductile polymer. Although the maximum elongation of **PP-LDPE-SS-5** is significantly lower than **LDPE-SS-5**, this may potentially be attributed to stabilizers and plasticizers commonly added to consumer plastics. A similar decrease in elongation was observed when Nicolaÿ *et al.* compared reactive crosslinking of postconsumer waste versus a virgin PP-LDPE blend with their azidotriazine crosslinker.[44]

Nevertheless, we have demonstrated that the **SS** crosslinker can crosslink a blend of used PP and LDPE plastic waste, imparting solvent resistance and ductility, even in the presence of stabilizers and plasticizers. This presents a promising route to upcycling plastic waste, potentially alleviating the production of plastic waste, which has become a global environmental burden in the past decade.[5–8] Further work can be done to investigate processing techniques which could improve the properties of these CANs from postconsumer plastics, as well as their mechanical and chemical recyclability.

Conclusion

In conclusion, our work has demonstrated an *in-situ* approach to crosslinking commodity thermoplastics with dynamic covalent crosslinkers bearing PFPA groups. Three different dynamic covalent crosslinkers – **SS**, **Im** and **SpA** – were synthesized in 2 steps and high yield. The PFPA groups were activated at ~160 °C to form reactive nitrenes which performed C-H insertion into various polymers to form covalent adaptable networks, which displayed excellent dimensional stability and solvent resistance compared to their original thermoplastics. In particular, the disulfide vitrimer **LDPE-SS-5** exhibited stress relaxation properties which was tunable by addition of $POct_3$ catalyst, enabling self-healing and mechanical recycling of the vitrimers. Notably, **LDPE-SS-5** showed superior maximum elongation compared to **LDPE control**, and could retain these properties even after 5 recycles. Additionally, both **LDPE-SS** and **LDPE-SpA** CANs could be chemically recycled via hot solvent and catalyst addition into its un-crosslinked state (thermoplastic), followed by re-crosslinking to reform the CAN in a vacuum oven. Finally, we also demonstrated that the **SS** crosslinker could upcycle a blend of postconsumer poly(olefin) (LDPE:PP = 70:30 w/w) waste into vitrimers with enhanced mechanical

properties. Despite the dark colour post-crosslinking, we envisage that our approach of transforming thermoplastics into healable and recyclable CANs could significantly improve plastics circularity, contributing towards the United Nations Sustainable Development Goals (UN SDG) 12.5 of substantially reducing waste generation through reduction, prevention, reuse and recycling. Additionally, the ability to upcycle waste plastic feedstock into CANs with high-value applications is in line also in line with the goals of combating resource depletion (UN SDG 12.2) and reducing greenhouse gas emissions from incineration (UN SDG 13.2).

Experimental procedures

Full experimental procedures are available in the supplemental information.

Resource availability

Lead contact

Further information and requests for resources should be directed to and will be fulfilled by the lead contact, Shermin S. Goh (gohsms@imre.a-star.edu.sg).

Materials availability

All unique materials generated in this study will be made available on request, but we may require a payment and/or a completed materials transfer agreement if there is potential for commercial application.

Data and code availability

Full experimental procedures are available in the supplemental information.

Document S1. Full experimental procedures, graphs and spectra

Video S1. Video of **LDPE-SS-5**

Acknowledgements

The authors would like to acknowledge Dr. Tristan Tan for his help with XRD, Dr. Hazel Lau for her help with HRMS, Ms. Rachel Lau for her help with gel fraction experiments, Ms. Xi Ping Ni for her help with DSC and Mr. Marcus Lim for his help with artwork. This research is supported by A*STAR under its Manufacturing, Trade And Connectivity (MTC) Programmatic Fund (M22K9b0049).

Author Contributions

Z.Y.L. and S.K. contributed equally. Conceptualization: Z.M.P. and S.S.G.; Investigation: Z.Y.L., S.K., R.R., S.Y.X.S., G.E.K.K.S, A.W.G. and S.S.G; Writing – original draft: Z.Y.L., S.K. and Z.M.P.; Writing – reviewing & editing: Z.L., Z.M.P. and S.S.G.; Funding: S.S.G. and Z. Li; Supervision: S.S.G.

Declaration of Interests

Z.M. Png, S.S. Goh, Z.Y. Lee and S. Kamarulzaman are listed as inventors on a patent application based on the results presented herein.

References:

(1) Zheng, J.; Png, Z. M.; Ng, S. H.; Tham, G. X.; Ye, E.; Goh, S. S.; Loh, X. J.; Li, Z. Vitrimers: Current Research Trends and Their Emerging Applications. *Mater. Today* **2021**, *51*, 586–625. https://doi.org/10.1016/J.MATTOD.2021.07.003.

(2) Kamarulzaman, S.; Png, Z. M.; Lim, E. Q.; Lim, I. Z. S.; Li, Z.; Goh, S. S. Covalent Adaptable Networks from Renewable Resources: Crosslinked Polymers for a Sustainable Future. *Chem* **2023**, *9* (10), 2771–2816.

https://doi.org/10.1016/J.CHEMPR.2023.04.024.
(3) Denissen, W.; Winne, J. M.; Du Prez, F. E. Vitrimers: Permanent Organic Networks with Glass-like Fluidity. *Chem. Sci.* **2016**, *7* (1), 30–38. https://doi.org/10.1039/c5sc02223a.
(4) Winne, J. M.; Leibler, L.; Du Prez, F. E. Dynamic Covalent Chemistry in Polymer Networks: A Mechanistic Perspective. *Polym. Chem.* **2019**, *10* (45), 6091–6108. https://doi.org/10.1039/c9py01260e.
(5) Williams, M.; Gower, R.; Green, J. *No Time to Waste. Tackling the Plastic Pollution Crisis Before It's Too Late*; 2019.
(6) OECD. *Global Plastics Outlook*; OECD, 2022. https://doi.org/10.1787/de747aef-en.
(7) Borrelle, S. B.; Ringma, J.; Lavender Law, K.; Monnahan, C. C.; Lebreton, L.; McGivern, A.; Murphy, E.; Jambeck, J.; Leonard, G. H.; Hilleary, M. A.; Eriksen, M.; Possingham, H. P.; De Frond, H.; Gerber, L. R.; Polidoro, B.; Tahir, A.; Bernard, M.; Mallos, N.; Barnes, M.; Rochman, C. M. Predicted Growth in Plastic Waste Exceeds Efforts to Mitigate Plastic Pollution. *Science* **2020**, *369* (6509), 1515–1518. https://doi.org/10.1126/SCIENCE.ABA3656.
(8) Stegmann, P.; Daioglou, V.; Londo, M.; van Vuuren, D. P.; Junginger, M. Plastic Futures and Their CO2 Emissions. *Nature* **2022**, *612* (7939), 272–276. https://doi.org/10.1038/s41586-022-05422-5.
(9) United Nations Environment Programme. *Turning off the Tap. How the World Can End Plastic Pollution and Create a Circular Economy*; Nairobi, 2023.
(10) Bachmann, M.; Zibunas, C.; Hartmann, J.; Tulus, V.; Suh, S.; Guillén-Gosálbez, G.; Bardow, A. Towards Circular Plastics within Planetary Boundaries. *Nat. Sustain.* **2023**, *6* (5), 599–610. https://doi.org/10.1038/s41893-022-01054-9.
(11) Guerre, M.; Taplan, C.; Winne, J. M.; Du Prez, F. E. Vitrimers: Directing Chemical Reactivity to Control Material Properties. *Chem. Sci.* **2020**, *11* (19), 4855–4870. https://doi.org/10.1039/d0sc01069c.
(12) Gao, H.; Sun, Y.; Wang, M.; Wang, Z.; Han, G.; Jin, L.; Lin, P.; Xia, Y.; Zhang, K. Mechanically Robust and Reprocessable Acrylate Vitrimers with Hydrogen-Bond-Integrated Networks for Photo-3D Printing. *ACS Appl. Mater. Interfaces* **2020**. https://doi.org/10.1021/acsami.0c19520.
(13) Zhong, L.; Hao, Y.; Zhang, J.; Wei, F.; Li, T.; Miao, M.; Zhang, D. Closed-Loop Recyclable Fully Bio-Based Epoxy Vitrimers from Ferulic Acid-Derived Hyperbranched Epoxy Resin. *Macromolecules* **2022**, *55* (2), 595–607. https://doi.org/10.1021/acs.macromol.1c02247.
(14) Png, Z. M.; Zheng, J.; Kamarulzaman, S.; Wang, S.; Li, Z.; Goh, S. S. Fully Biomass-Derived Vitrimeric Material with Water-Mediated Recyclability and Monomer Recovery. *Green Chem.* **2022**, *24* (15), 5978–5986. https://doi.org/10.1039/D2GC01556K.
(15) Saito, K.; Eisenreich, F.; Türel, T.; Tomović, Ž. Closed-Loop Recycling of Poly(Imine-Carbonate) Derived from Plastic Waste and Bio-Based Resources. *Angew. Chemie Int. Ed.* **2022**, *61* (43), e202211806. https://doi.org/https://doi.org/10.1002/anie.202211806.
(16) Chen, L.; Malollari, K. G.; Uliana, A.; Sanchez, D.; Messersmith, P. B.; Hartwig, J. F. Selective, Catalytic Oxidations of C-H Bonds in Polyethylenes Produce Functional Materials with Enhanced Adhesion. *Chem* **2021**, *7* (1), 137–145. https://doi.org/10.1016/j.chempr.2020.11.020.
(17) Ciccia, N. R.; Shi, J. X.; Pal, S.; Hua, M.; Malollari, K. G.; Lizandara-Pueyo, C.; Risto, E.; Ernst, M.; Helms, B. A.; Messersmith, P. B.; Hartwig, J. F. Diverse Functional Polyethylenes by Catalytic Amination. *Science* **2023**, *381* (6665), 1433–

1440. https://doi.org/10.1126/science.adg6093.
(18) Caffy, F.; Nicolaÿ, R. Transformation of Polyethylene into a Vitrimer by Nitroxide Radical Coupling of a Bis-Dioxaborolane. *Polym. Chem.* **2019**, *10* (23), 3107–3115. https://doi.org/10.1039/c9py00253g.
(19) Maaz, M.; Riba-Bremerch, A.; Guibert, C.; Van Zee, N. J.; Nicolaÿ, R. Synthesis of Polyethylene Vitrimers in a Single Step: Consequences of Graft Structure, Reactive Extrusion Conditions, and Processing Aids. *Macromolecules* **2021**, *54* (5), 2213–2225. https://doi.org/10.1021/ACS.MACROMOL.0C02649.
(20) Li, Z.; Wen, Y.; Song, Z.; Zhang, C.; Cui, C.; An, D.; Ge, Z.; Cheng, Y.; Zhang, Q.; Zhang, Y. Dynamic Cross-Linked Polyethylene Networks with High Energy Storage and Electrical Damage Self-Healability. *ACS Macro Lett.* **2023**, *12* (10), 1409–1415. https://doi.org/10.1021/acsmacrolett.3c00394.
(21) Neidhart, E. K.; Hua, M.; Peng, Z.; Kearney, L. T.; Bhat, V.; Vashahi, F.; Alexanian, E. J.; Sheiko, S. S.; Wang, C.; Helms, B. A.; Leibfarth, F. A. C–H Functionalization of Polyolefins to Access Reprocessable Polyolefin Thermosets. *J. Am. Chem. Soc.* **2023**, *145* (50), 27450–27458. https://doi.org/10.1021/jacs.3c08682.
(22) Kar, G. P.; Saed, M. O.; Terentjev, E. M. Scalable Upcycling of Thermoplastic Polyolefins into Vitrimers through Transesterification. *J. Mater. Chem. A* **2020**, *8* (45), 24137–24147. https://doi.org/10.1039/D0TA07339C.
(23) Lepage, M. L.; Simhadri, C.; Liu, C.; Takaffoli, M.; Bi, L.; Crawford, B.; Milani, A. S.; Wulff, J. E. A Broadly Applicable Cross-Linker for Aliphatic Polymers Containing C–H Bonds. *Science* **2019**, *366* (6467), 875–878. https://doi.org/10.1126/science.aay6230.
(24) Bi, L.; Godwin, B.; Baran, M. J.; Nazir, R.; Wulff, J. E. A Cleavable Crosslinking Strategy for Commodity Polymer Functionalization and Generation of Reprocessable Thermosets. *Angew. Chemie Int. Ed.* **2023**, *62* (30), e202304708. https://doi.org/10.1002/ANIE.202304708.
(25) Clarke, R. W.; Sandmeier, T.; Franklin, K. A.; Reich, D.; Zhang, X.; Vengallur, N.; Patra, T. K.; Tannenbaum, R. J.; Adhikari, S.; Kumar, S. K.; Rovis, T.; Chen, E. Y. X. Dynamic Crosslinking Compatibilizes Immiscible Mixed Plastics. *Nature* **2023**, *616* (7958), 731–739. https://doi.org/10.1038/S41586-023-05858-3.
(26) Song, M.-G.; Sheridan, R. S. Effects of CF3 Groups and Charged Substituents on Singlet Carbene Stabilities–a Density Functional Theory Study. *J. Phys. Org. Chem.* **2011**, *24* (10), 889–893. https://doi.org/10.1002/poc.1913.
(27) Breuillac, A.; Caffy, F.; Vialon, T.; Nicolaÿ, R. Functionalization of Polyisoprene and Polystyrene via Reactive Processing Using Azidoformate Grafting Agents, and Its Application to the Synthesis of Dioxaborolane-Based Polyisoprene Vitrimers. *Polym. Chem.* **2020**, *11* (40), 6479–6491. https://doi.org/10.1039/D0PY00164C.
(28) Poe, R.; Schnapp, K.; Young, M. J. T.; Grayzar, J.; Platz, M. S. Chemistry and Kinetics of Singlet Pentafluorophenylnitrene. *J. Am. Chem. Soc.* **1992**, *114* (13), 5054–5067. https://doi.org/10.1021/ja00039a016.
(29) Marcinek, A.; Platz, M. S.; Chan, S. Y.; Floresca, R.; Rajagopalan, K.; Golinski, M.; Watt, D. Unusually Long Lifetimes of the Singlet Nitrenes Derived from 4-Azido-2,3,5,6-Tetrafluorobenzamides. *J. Phys. Chem.* **1994**, *98* (2), 412–419. https://doi.org/10.1021/j100053a012.
(30) Gritsan, N. P.; Gudmundsdóttir, A. D.; Tigelaar, D.; Zhu, Z.; Karney, W. L.; Hadad, C. M.; Platz, M. S. A Laser Flash Photolysis and Quantum Chemical Study of the Fluorinated Derivatives of Singlet Phenylnitrene. *J. Am. Chem. Soc.* **2001**, *123* (9), 1951–1962. https://doi.org/10.1021/ja9944305.
(31) Png, R.-Q.; Chia, P.-J.; Tang, J.-C.; Liu, B.; Sivaramakrishnan, S.; Zhou, M.; Khong,

S.-H.; Chan, H. S. O.; Burroughes, J. H.; Chua, L.-L.; Friend, R. H.; Ho, P. K. H. High-Performance Polymer Semiconducting Heterostructure Devices by Nitrene-Mediated Photocrosslinking of Alkyl Side Chains. *Nat. Mater.* **2010**, *9* (2), 152–158. https://doi.org/10.1038/nmat2594.

(32) Cai, S. X.; Glenn, D. J.; Kanska, M.; Wybourne, M. N.; Keana, J. F. W. Development of Highly Efficient Deep-UV and Electron Beam Mediated Cross-Linkers: Synthesis and Photolysis of Bis(Perfluorophenyl) Azides. *Chem. Mater.* **1994**, *6* (10), 1822–1829. https://doi.org/10.1021/CM00046A041.

(33) Keana, J. F. W.; Cai, S. X. New Reagents for Photoaffinity Labeling: Synthesis and Photolysis of Functionalized Perfluorophenyl Azides. *J. Org. Chem.* **1990**, *55* (11), 3640–3647. https://doi.org/10.1021/jo00298a048.

(34) Tan, Z.-S.; Jamal, Z.; Teo, D. W. Y.; Ko, H.-C.; Seah, Z.-L.; Phua, H.-Y.; Ho, P. K. H.; Png, R.-Q.; Chua, L.-L. Optimization of Fluorinated Phenyl Azides as Universal Photocrosslinkers for Semiconducting Polymers. *Nat. Commun.* **2024**, *15* (1), 6354. https://doi.org/10.1038/s41467-024-50257-5.

(35) Wang, D.; Ding, J.; Ma, Y.; Xu, C.; Li, Z.; Zhang, X.; Zhao, Y.; Zhao, Y.; Di, Y.; Liu, L.; Dai, X.; Zou, Y.; Kim, B.; Zhang, F.; Liu, Z.; McCulloch, I.; Lee, M.; Chang, C.; Yang, X.; Wang, D.; Zhang, D.; Zhao, L.-D.; Di, C.; Zhu, D. Multi-Heterojunctioned Plastics with High Thermoelectric Figure of Merit. *Nature* **2024**, *632* (8025), 528–535. https://doi.org/10.1038/s41586-024-07724-2.

(36) Teo, D. W. Y.; Jamal, Z.; Phua, H. Y.; Tang, C. G.; Png, R. Q.; Chua, L. L. Nearly 100% Photocrosslinking Efficiency in Ultrahigh Work Function Hole-Doped Conjugated Polymers Using Bis(Fluorophenyl Azide) Additives. *ACS Appl. Mater. Interfaces* **2019**, *11* (51), 48103–48112. https://doi.org/10.1021/ACSAMI.9B12503.

(37) Musolino, S. F.; Pei, Z.; Bi, L.; DiLabio, G. A.; Wulff, J. E. Structure–Function Relationships in Aryl Diazirines Reveal Optimal Design Features to Maximize C–H Insertion. *Chem. Sci.* **2021**. https://doi.org/10.1039/D1SC03631A.

(38) Png, Z. M.; Goh, S. S.; Lee, Z. Y.; Kamarulzaman, S. A Dynamic Crosslinker, Covalent Adaptable Network Comprising Polymer Network Crosslinked by Said Dynamic Crosslinker and Related Methods Thereof. PCT/SG2024/050606, 2024.

(39) Bhat, V. T.; James, N. R.; Jayakrishnan, A. A Photochemical Method for Immobilization of Azidated Dextran onto Aminated Poly(Ethylene Terephthalate) Surfaces. *Polym. Int.* **2008**, *57* (1), 124–132. https://doi.org/10.1002/pi.2332.

(40) Niklas Lorenz; E. Dyer, W.; Baris Kumru. Thermo-Rheological and Kinetic Characterization and Modeling of an Epoxy Vitrimer Based on Polyimine Exchange. *Soft Matter* **2024**, *20* (31), 6289–6301. https://doi.org/10.1039/D4SM00724G.

(41) Dodd, L. J.; Lima, C.; Costa-Milan, D.; Neale, A. R.; Saunders, B.; Zhang, B.; Sarua, A.; Goodacre, R.; Hardwick, L. J.; Kuball, M.; Hasell, T. Raman Analysis of Inverse Vulcanised Polymers. *Polym. Chem.* **2023**, *14* (12), 1369–1386. https://doi.org/10.1039/D2PY01408D.

(42) Jia, Y.; Zhang, H.; Zhang, J. The Effect of Peroxide Cross-Linking on the Thermal Conductivity and Crystallinity of Low-Density Polyethylene. *Mater. Today Commun.* **2022**, *31*, 103735. https://doi.org/10.1016/J.MTCOMM.2022.103735.

(43) United Nations Environment Programme. *Addressing Single-Use Plastic Products Pollution Using a Life Cycle Approach*; Nairobi, 2021.

(44) Vialon, T.; Sun, H.; Formon, G. J. M.; Galanopoulo, P.; Guibert, C.; Averseng, F.; Rager, M. N.; Percot, A.; Guillaneuf, Y.; Van Zee, N. J.; Nicolaÿ, R. Upcycling Polyolefin Blends into High-Performance Materials by Exploiting Azidotriazine Chemistry Using Reactive Extrusion. *J. Am. Chem. Soc.* **2024**, *146* (4), 2673–2684. https://doi.org/10.1021/JACS.3C12303.

(45) Pepels, M.; Filot, I.; Klumperman, B.; Goossens, H. Self-Healing Systems Based on Disulfide-Thiol Exchange Reactions. *Polym. Chem.* **2013**, *4* (18), 4955–4965. https://doi.org/10.1039/c3py00087g.
(46) Ruiz de Luzuriaga, A.; Solera, G.; Azcarate-Ascasua, I.; Boucher, V.; Grande, H. J.; Rekondo, A. Chemical Control of the Aromatic Disulfide Exchange Kinetics for Tailor-Made Epoxy Vitrimers. *Polymer (Guildf).* **2022**, *239*, 124457. https://doi.org/10.1016/J.POLYMER.2021.124457.
(47) Matxain, J. M.; Asua, J. M.; Ruipérez, F. Design of New Disulfide-Based Organic Compounds for the Improvement of Self-Healing Materials. *Phys. Chem. Chem. Phys.* **2016**, *18* (3), 1758–1770. https://doi.org/10.1039/C5CP06660C.
(48) Van Lijsebetten, F.; De Bruycker, K.; Van Ruymbeke, E.; Winne, J. M.; Du Prez, F. E. Characterising Different Molecular Landscapes in Dynamic Covalent Networks. *Chem. Sci.* **2022**, *13* (43), 12865–12875. https://doi.org/10.1039/D2SC05528G.
(49) Martins, M. L.; Zhao, X.; Demchuk, Z.; Luo, J.; Carden, G. P.; Toleutay, G.; Sokolov, A. P. Viscoelasticity of Polymers with Dynamic Covalent Bonds: Concepts and Misconceptions. *Macromolecules* **2023**, *56* (21), 8688–8696. https://doi.org/10.1021/ACS.MACROMOL.3C01545.
(50) Ricarte, R. G.; Shanbhag, S. A Tutorial Review of Linear Rheology for Polymer Chemists: Basics and Best Practices for Covalent Adaptable Networks. *Polym. Chem.* **2024**, *15* (9), 815–846. https://doi.org/10.1039/D3PY01367G.
(51) Caraballo, R.; Rahm, M.; Vongvilai, P.; Brinck, T.; Ramström, O. Phosphine-Catalyzed Disulfide Metathesis. *Chem. Commun.* **2008**, No. 48, 6603–6605. https://doi.org/10.1039/B815710C.
(52) Lei, Z. Q.; Xiang, H. P.; Yuan, Y. J.; Rong, M. Z.; Zhang, M. Q. Room-Temperature Self-Healable and Remoldable Cross-Linked Polymer Based on the Dynamic Exchange of Disulfide Bonds. *Chem. Mater.* **2014**, *26* (6), 2038–2046. https://doi.org/10.1021/CM4040616.
(53) Nevejans, S.; Ballard, N.; Miranda, J. I.; Reck, B.; Asua, J. M. The Underlying Mechanisms for Self-Healing of Poly(Disulfide)S. *Phys. Chem. Chem. Phys.* **2016**, *18* (39), 27577–27583. https://doi.org/10.1039/c6cp04028d.
(54) Jourdain, A.; Asbai, R.; Anaya, O.; Chehimi, M. M.; Drockenmuller, E.; Montarnal, D. Rheological Properties of Covalent Adaptable Networks with 1,2,3-Triazolium Cross-Links: The Missing Link between Vitrimers and Dissociative Networks. *Macromolecules* **2020**, *53* (6), 1884–1900. https://doi.org/10.1021/acs.macromol.9b02204.
(55) Du, Y.; Wang, D. One-Pot Preparation of Double-Network Epoxy Vitrimers with High Performance, Recyclability, and Two-Stage Stress Relaxation. *ACS Appl. Mater. Interfaces* **2024**, *16* (31), 41551–41561. https://doi.org/10.1021/ACSAMI.4C09123.
(56) Pawelec, W.; Holappa, A.; Tirri, T.; Aubert, M.; Hoppe, H.; Pfaendner, R.; Wilén, C. E. Disulfides - Effective Radical Generators for Flame Retardancy of Polypropylene. *Polym. Degrad. Stab.* **2014**, *110*, 447–456. https://doi.org/10.1016/j.polymdegradstab.2014.09.013.
(57) Singh, B.; Sharma, N. Mechanistic Implications of Plastic Degradation. *Polym. Degrad. Stab.* **2008**, *93* (3), 561–584. https://doi.org/10.1016/j.polymdegradstab.2007.11.008.
(58) Jin, H.; Gonzalez-Gutierrez, J.; Oblak, P.; Zupančič, B.; Emri, I. The Effect of Extensive Mechanical Recycling on the Properties of Low Density Polyethylene. *Polym. Degrad. Stab.* **2012**, *97* (11), 2262–2272. https://doi.org/10.1016/j.polymdegradstab.2012.07.039.
(59) Saikrishnan, S.; Jubinville, D.; Tzoganakis, C.; Mekonnen, T. H. Thermo-Mechanical

Degradation of Polypropylene (PP) and Low-Density Polyethylene (LDPE) Blends Exposed to Simulated Recycling. *Polym. Degrad. Stab.* **2020**, *182*, 109390. https://doi.org/https://doi.org/10.1016/j.polymdegradstab.2020.109390.
(60) Mendes, A. A.; Cunha, A. M.; Bernardo, C. A. Study of the Degradation Mechanisms of Polyethylene during Reprocessing. *Polym. Degrad. Stab.* **2011**, *96* (6), 1125–1133. https://doi.org/https://doi.org/10.1016/j.polymdegradstab.2011.02.015.
(61) Gugumus, F. Physico-Chemical Aspects of Polyethylene Processing in an Open Mixer 2. Functional Group Formation on PE–LD Processing. *Polym. Degrad. Stab.* **2000**, *67* (1), 35–47. https://doi.org/https://doi.org/10.1016/S0141-3910(99)00115-9.
(62) Png, Z. M.; Wang, S.; Yeo, J. C. C.; Raveenkumar, V.; Muiruri, J. K.; Quek, X. C. N.; Yu, X.; Li, K.; Li, Z. Reversible Vitrimisation of Single-Use Plastics and Their Mixtures. *Adv. Funct. Mater.* **2024**, 2410291. https://doi.org/10.1002/ADFM.202410291.
(63) Sakai, T. Experimental Verification of Homogeneity in Polymer Gels. *Polym. J.* **2014**, *46* (9), 517–523. https://doi.org/10.1038/pj.2014.28.
(64) Greenlee, A. J.; Wendell, C. I.; Cencer, M. M.; Laffoon, S. D.; Moore, J. S. Kinetic and Thermodynamic Control in Dynamic Covalent Synthesis. *Trends Chem.* **2020**, *2* (12), 1043–1051. https://doi.org/10.1016/J.TRECHM.2020.09.005.
(65) Lemcoff, N. G.; Fuchs, B. Toward Novel Polyacetals by Transacetalation Techniques: Dendrimeric Diacetals. *Org. Lett.* **2002**, *4* (5), 731–734. https://doi.org/10.1021/OL017230I.
(66) Yu, S.; Wu, S.; Zhang, C.; Tang, Z.; Luo, Y.; Guo, B.; Zhang, L. Catalyst-Free Metathesis of Cyclic Acetals and Spirocyclic Acetal Covalent Adaptable Networks. *ACS Macro Lett.* **2020**, *9* (8), 1143–1148. https://doi.org/10.1021/ACSMACROLETT.0C00527.
(67) Li, Q.; Ma, S.; Wang, S.; Yuan, W.; Xu, X.; Wang, B.; Huang, K.; Zhu, J. Facile Catalyst-Free Synthesis, Exchanging, and Hydrolysis of an Acetal Motif for Dynamic Covalent Networks. *J. Mater. Chem. A* **2019**, *7* (30), 18039–18049. https://doi.org/10.1039/c9ta04073k.
(68) Li, Q.; Ma, S.; Wang, S.; Liu, Y.; Taher, M. A.; Wang, B.; Huang, K.; Xu, X.; Han, Y.; Zhu, J. Green and Facile Preparation of Readily Dual-Recyclable Thermosetting Polymers with Superior Stability Based on Asymmetric Acetal. *Macromolecules* **2020**, *53* (4), 1474–1485. https://doi.org/10.1021/ACS.MACROMOL.9B02386.
(69) Li, Q.; Ma, S.; Li, P.; Wang, B.; Feng, H.; Lu, N.; Wang, S.; Liu, Y.; Xu, X.; Zhu, J. Biosourced Acetal and Diels-Alder Adduct Concurrent Polyurethane Covalent Adaptable Network. *Macromolecules* **2021**, *54* (4), 1742–1753. https://doi.org/10.1021/acs.macromol.0c02699.
(70) Matsukizono, H.; Endo, T. Reworkable Polyhydroxyurethane Films with Reversible Acetal Networks Obtained from Multifunctional Six-Membered Cyclic Carbonates. *J. Am. Chem. Soc.* **2018**, *140* (3), 884–887. https://doi.org/10.1021/jacs.7b11824.
(71) Ma, S.; Wei, J.; Jia, Z.; Yu, T.; Yuan, W.; Li, Q.; Wang, S.; You, S.; Liu, R.; Zhu, J. Readily Recyclable, High-Performance Thermosetting Materials Based on a Lignin-Derived Spiro Diacetal Trigger. *J. Mater. Chem. A* **2019**, *7* (3), 1233–1243. https://doi.org/10.1039/C8TA07140C.
(72) Geyer, R.; Jambeck, J. R.; Law, K. L. Production, Use, and Fate of All Plastics Ever Made. *Sci. Adv.* **2017**, *3* (7). https://doi.org/10.1126/SCIADV.1700782.
(73) Chanda, M.; Roy, S. K. *Plastics Fabrication and Recycling*; CRC Press: Boca Raton, 2008. https://doi.org/10.1201/9781420080636.